

# THE EFFECTS OF MECHANICAL FORCES ON BONES AND JOINTS

## EXPERIMENTAL STUDY ON THE RAT TAIL

UGO E. PAZZAGLIA, LUCA ANDRINI, AMALIA DI NUCCI

*From the University of Pavia, Varese, Italy*

**We have used an experimental model employing the bent tail of rats to investigate the effects of mechanical forces on bones and joints. Mechanical strain could be applied to the bones and joints of the tail without direct surgical exposure or the application of pins and wires.**

**The intervertebral disc showed stretched annular lamellae on the convex side, while the annulus fibrosus on the concave side was pinched between the inner corners of the vertebral epiphysis. In young rats with an active growth plate, a transverse fissure appeared at the level of the hypertrophic cell layer or the primary**

**An explanation of the phenomena capable of influencing the shape and architecture of the skeleton has been provided by 'Wolff's law'<sup>1-3</sup> and by the chondral modelling theory.<sup>4</sup> These theories are supported by anatomical and developmental studies and also by clinical experience. Although Wolff's law is accepted in orthopaedics, there have been few morphometric studies, and their results are controversial.<sup>5-9</sup> Most models are complicated by the use of surgical procedures and mechanical devices which interfere with the changes under study. The rat tail therefore is a suitable model for studying the effects of mechanical forces**

**thicker and more dense than those of the distracted part of the vertebra.**

**In growing animals, morphometric analysis of hemiepiphyseal and hemimetaphyseal areas, and the corresponding trabecular bone density, showed significant differences between the compressed and distracted sides. No differences were observed in adult rats. We found no significant differences in osteoclast number between compressed and distracted sides in either age group. Our results provide quantitative evidence of the working of 'Wolff's law'.**

**The differences in trabecular density are examples of remodelling by osteoclasts and osteoblasts; our finding of no significant difference in osteoclast numbers between the hemiepiphyses in the experimental and control groups suggests that the response of living bone to altered strain is mediated by osteoblasts.**

*J Bone Joint Surg [Br] 1997;79-B:1024-30.*

*Received 10 March 1997; Accepted after revision 9 May 1997*

---

U. E. Pazzaglia, MD, Professor of Orthopaedic Surgery  
2 Divisione di Ortopedia e Traumatologia, Spedali Civili, 1-25125 Brescia, Italy.

L. Andrini, MD, Registrar  
Clinica Ortopedica, Università di Pavia, 1-21100 Varese, Italy.

A. Di Nucci, BiolD, Researcher  
Istituto di Farmacologia II, Università di Pavia, Italy.

Correspondence should be sent to Professor U. E. Pazzaglia.

---

©1997 British Editorial Society of Bone and Joint Surgery  
0301-620X/97/67749 \$2.00

**This model has been used in studies on bone modelling in which bent tails were implanted in extraskeletal sites of the same rat or syngenic animals.<sup>10-12</sup> Our aim was to use the rat tail to study the response of living bones and joints to mechanical forces.**

## MATERIALS AND METHODS

We used 48 male Sprague-Dawley rats divided into two groups of 24. The first group was young rats with a mean weight of 118 g. In 12 animals we tied the tail with a metal wire to form a loop, which included 14 vertebrae (Fig. 1). Six rats were killed after 30 days and six after 90 days. The remaining 12 rats, with their tail left free, were the control group and were killed at the same time intervals. The second group were adult rats, with a mean weight of 450 g, which were studied in the same way. In anaesthetised animals, we used a dynamometer to measure the force required to close a loop including two-thirds of the total length of the tail (Table I).

Two animals were kept in each cage, with free access to food and water, and all were given tetracycline 30 mg/kg/day intraperitoneally for seven days before they were killed with an overdose of ether. Two animals in each of the experimental and control groups (total 16) had perfusion of the vascular tree of the hind limb and tail with a solution of black Indian ink through the abdominal aorta.

The tail was severed and plain AP radiographs taken. The overlying skin was removed, and the tail fixed in a solution of neutral formalin (10%). In each of the two

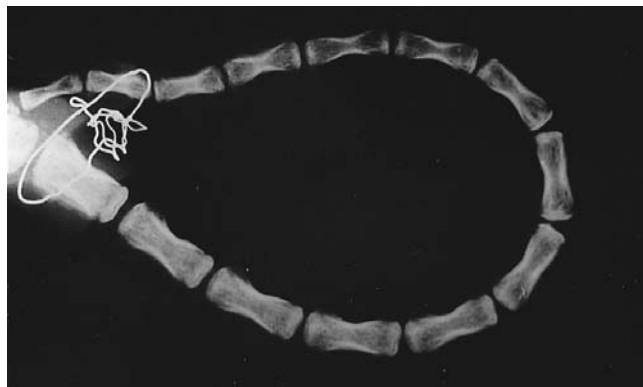


Fig. 1

Radiograph in the horizontal plane showing the tail loop of 14 vertebrae in an old rat.

experimental groups of six at each time interval, the tails of the two rats with Indian ink injection, and of two not injected were decalcified in EDTA solution (10%) for 20 days and embedded in paraffin. The other two tails were embedded undecalcified in methylmethacrylate resin. For the control groups, the tail of only one rat was embedded in resin (Table II).

Specimens were orientated in the horizontal plane using two pins placed through the sixth and eighth vertebrae. Histological sections were made in the plane of the loop and in the horizontal plane of unbent tails. Five consecutive median coronal sections were obtained of the vertebra at the apex of the loop (the seventh tail vertebra) with sections of the proximal and distal intervertebral discs. The corresponding vertebra of the control groups was also sectioned. Serial sections, in a plane perpendicular to the major axis of the seventh tail vertebra, were obtained from one injected control animal in each of the old and young groups (Table II).

Decalcified sections were stained with haematoxylin and eosin and used for morphometric evaluation. Paraffin-embedded sections were stained using the avidin-biotin-peroxidase complex technique,<sup>13</sup> for KP1 monoclonal antibody (Dako, Denmark) and also evaluated morphometrically. For descriptive morphology, sections 50  $\mu\text{m}$  thick of undecalcified, methylmethacrylate-embedded specimens were prepared by grinding. Undecalcified, resin-embedded, sections were used for a fluorescence study.

Histomorphometric studies were made of the decalcified specimens, selecting the best section from each age group.

The total area of the hemiepiphysis and the hemimetaphysis (HMEA) of the compressed and distracted sides in the experimental groups, and of both sides in the control group, was measured at the cranial and caudal ends of the seventh vertebra. The reference area was delimited by the median longitudinal axis of the vertebra and by the perimeter of the bone; the lower limit was arbitrarily taken as a line parallel to the growth plate, at three times the thickness of the epiphysis from the proliferative layer, as measured

on the median longitudinal axis. The hemiepiphysal area (HEA) was defined by the median longitudinal axis, its perimeter, and the border of the growth plate on the side of the proliferative cell layer. The hemimetaphysal area (HMA) was then calculated as the difference between the HMEA and HEA (Fig. 2). The areas of trabecular and cortical bone in the hemiepiphysis (HEBA) and hemimetaphysis (HMBA) were then measured and expressed as percentages of HEA and HMA. The cartilage of the growth plate and the cartilaginous cores of primary metaphysal trabeculae were included in measurements of the trabecular bone area. All measurements were made manually on photographic prints (negative enlargement  $\times 100$ ; prints enlargement  $\times 5$ ) using a graphics tablet (Summasketch Plus; Summagraphics, Fairfield, Connecticut) coupled to an IBM personal computer with software developed by the authors.

We calculated the differences in hemiepiphysal and hemimetaphysal areas (HEA, HMA) and trabecular density (HEBA, HMBA) between the compressed and distracted sides; the results for each seventh vertebra are given as the mean of the results for the cranial and caudal ends. For the control groups, we calculated the same differences between the right and the left hemimetaphysis. The mean values from each experimental group were then compared with the corresponding control values using a three-way ANOVA test.

We identified osteoclasts as multinuclear cells inside a resorption lacuna which were stained by KP1 monoclonal antibody; their numbers in the compressed and distracted hemiepiphyses of the bent vertebrae were compared with those in the right and left hemiepiphyses of the control vertebrae, again using a three-way ANOVA test. The osteoclast count was the mean of those of the cranial and caudal hemiepiphyses.

**Table I.** The mean weight ( $\text{g} \pm \text{SD}$ ), tail length ( $\text{mm} \pm \text{SD}$ ) and force ( $\text{N} \pm \text{SD}$ ) required to close a loop of 14 vertebrae in the two groups of rats

	Number	Weight	Tail length	Force
Young	12	118.75 $\pm$ 11.70	154.17 $\pm$ 8.21	0.44 $\pm$ 0.04
Old	12	450 $\pm$ 29.85	221.25 $\pm$ 8.82	1.29 $\pm$ 0.12

**Table II.** Details of the experimental design for the two groups

	30 days*	90 days*
Young (n = 24)		
Tail bent	4 dc† + 2 ndc	4 dc† + 2 ndc
Control	5 dc‡ + 1 ndc	5 dc‡ + 1 ndc
Old (n = 24)		
Tail bent	4 dc† + 2 ndc	4 dc† + 2 ndc
Control	5 dc‡ + 1 ndc	5 dc‡ + 1 ndc

\* dc, decalcified and paraffin-embedded; ndc, undecalcified and methylmethacrylate-embedded

† two had the vascular tree of the hind limb and tail perfused with black Indian Ink solution (50%)

‡ one injected tail used for serial sections perpendicular to the tail axis

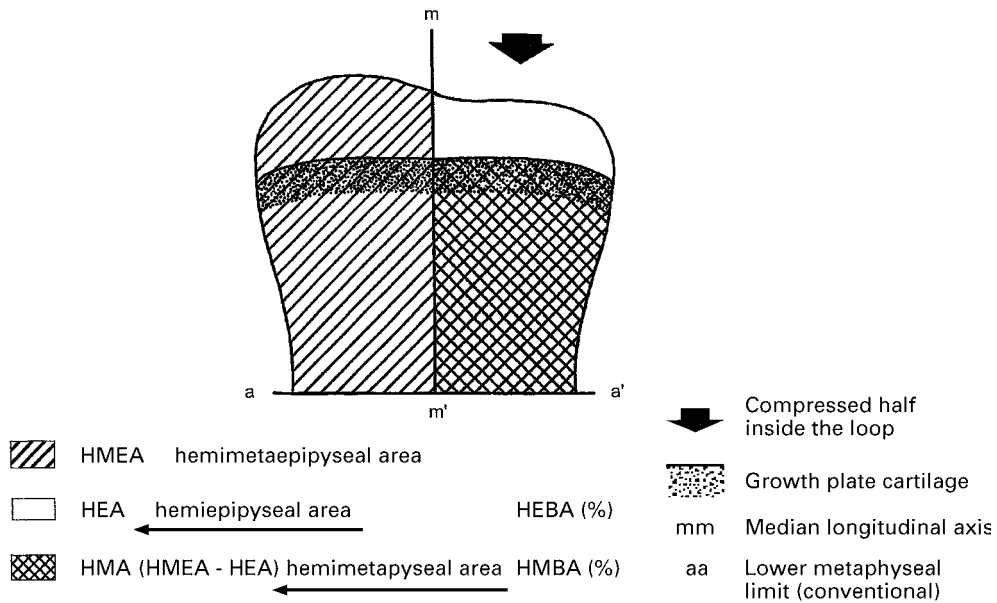


Fig. 2

Histomorphometric parameters evaluated on the median coronal section of the seventh tail vertebra.

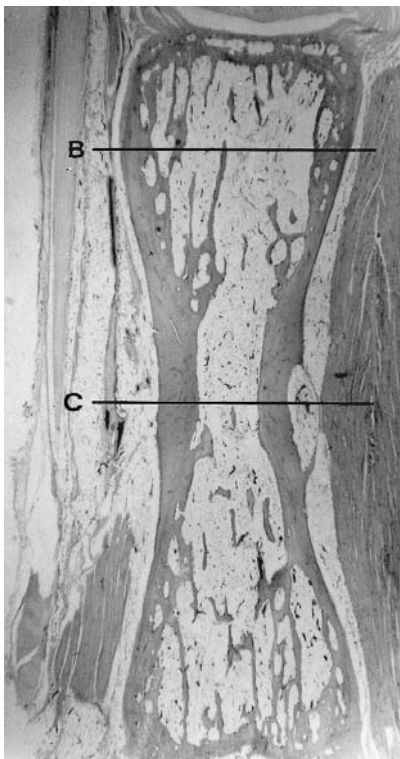


Fig. 3a

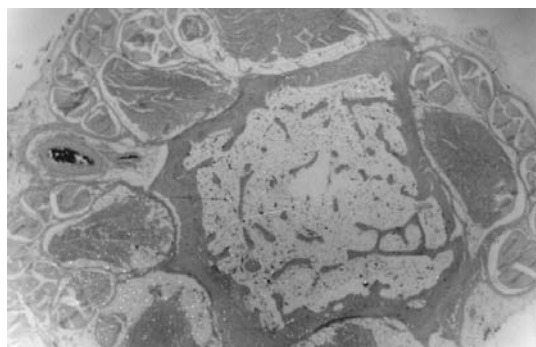


Fig. 3b

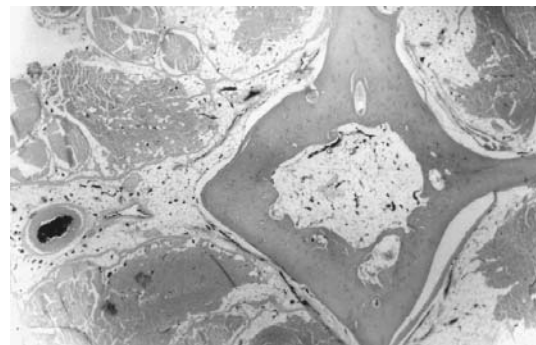


Fig. 3c

Figure 3a – General view of the seventh tail vertebra and surrounding soft tissue in the median coronal plane of a control rat ( $\times 7$ ). Figure 3b – Transverse section at the level of the metaphysis showing the homogeneous distribution of metaphyseal trabeculae ( $\times 18$ ). Figure 3c – Transverse section at the level of the diaphysis. On the left (ventral to the vertebra) the injected main artery of the tail is evident ( $\times 18$ ) (haematoxylin and eosin; vessels injected with Indian Ink).



Fig. 4

In the bent tail of a young rat (right), the fluorescent band of the growth plate appears more irregular than in the corresponding control rat (left). Small focal areas of fluorescence are present in the compressed epiphyses and metaphyses (tetracycline  $\times 3$ ).

## RESULTS

**Control tails.** The seventh tail vertebra has an egg-timer shape with thicker cortical bone in its middle (Fig. 3a). Both epiphyses and metaphyses are trabecular; the central part of the body is filled with adipose marrow tissue (Figs 3b and 3c). On the outer perimeter of the vertebral body there is a pronounced dorsal apophysis with two less developed apophyses on the right and left sides. A small protuberance extends ventrally (Fig. 3c). At the level of the metaphysis all these apophyses become less prominent (Fig. 3b). The main arterial supply enters the medullary cavity in the middle portion of the bone and branches proximally and distally, following the pattern typical of tubular bones;<sup>14,15</sup> additional small vessels enter the bone through the periosteum. This is a thin fibrous layer with flattened cells resting on the bone surface, which becomes more cellular near the metaphysis. There was little periosteal apposition in the control group, even in the growing rats, as shown by the thin band of fluorescence on the outer contour of the bone (Fig. 4). Other than size, we found no changes in the

general bone architecture with increased age.

In the young control group, tetracycline labelling showed a band of fluorescence corresponding to the calcifying zone of the growth plate. The metaphysis showed mild fluorescence which was uniformly distributed. A periosteal band was also present on the contour of the diaphysis (Fig. 4). There were no unusual features of labelling in the adult control group.

**Morphological changes in the bent tail.** The most obvious changes were in the intervertebral discs, but there were no significant differences between the young and old rats. On the convex side the lamellae of the annulus fibrosus appeared to be stretched and in a parallel arrangement; on the concave side the annulus was pinched between the inner corners of the vertebral epiphyses with the inner lamellae folded inside the disc. The nucleus pulposus was pushed outwards and protruded against the tail tendons (Fig. 5a). Proliferation of fibrous connective tissue was present outside the protruding annulus.

In all the vertebrae of the young group the growth cartilage showed a transverse fissure of variable length; this

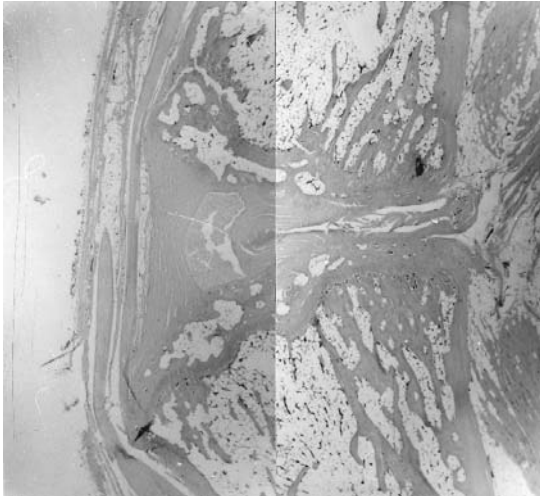


Fig. 5a

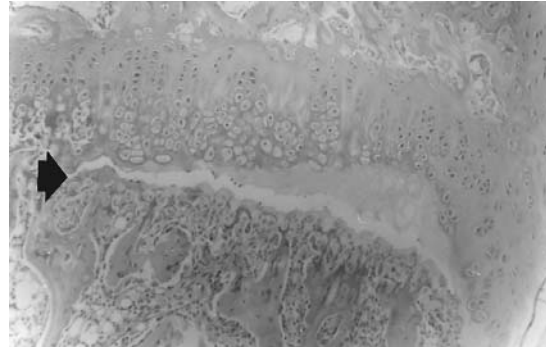


Fig. 5b

Figure 5a – The bent tail of a young rat after 90 days. The fibre of the annulus fibrosus and the nucleus pulposus is pushed outside. More dense epiphyseal and metaphyseal trabeculae are evident on the compressed side ( $\times 10$ ). Figure 5b – Fissuring of the growth plate cartilage is seen on the distracted side in a young rat ( $\times 20$ ) (haematoxylin and eosin).

was always in the tension half of the plate (Fig. 5b), and most often at the level of the hypertrophic cell layer at both ends of the bone. In a few, the cleft went through the primary metaphyseal trabecular zone. In the old rats there was no fracture of the cartilage.

In young rats, osteoblasts lined the surface of epiphyseal and metaphyseal trabeculae, but in the older rats the cells were flattened.

Young rats with bent tails had developed an unusual architectural arrangement of the epiphyseal and metaphyseal trabeculae on the compressed side at 90 days. The epiphyseal trabeculae were shorter and thicker, and the thickened metaphyseal trabeculae formed strong, oblique pillars between the growth plate and the cortex (Fig. 5a). No trabecular changes were seen in the older rats, and there were no changes in the cortical bone morphology of the diaphysis in either group.

In the bent-tail groups the fluorescent band of the growth plate appeared fragmented and irregular, with a notch at

the stretched corner of the vertebra. Fluorescent spots were scattered irregularly in the compressed epiphyses and metaphyses (Fig. 4). The metaphyseal trabeculae were more dense and more crowded on the concave than on the convex side of the tail. There were no significant changes in old rats.

**Morphometric changes in the bent tail.** The differences in the areas, both HEA and HMA, between compressed and distracted sides was significant after 90 days ( $p < 0.05$ ) in young rats with a bent tail compared with the corresponding control group. The changes in HEBA were significant after both 30 and 90 days ( $p < 0.01$ ) in the young rats. Changes in HMBA were significant at 90 days ( $p < 0.001$ ). There were no significant differences in old rats (Table III).

The mean number of osteoclasts in the compressed and the distracted areas of the hemiepiphysis in rats with bent tails and in the right and left hemiepiphysis of the control groups showed no significant differences between groups

**Table III.** Comparison of the hemiepiphyseal area (HEA), hemimetaphyseal area (HMA), hemiepiphyseal-bone-area (HEBA) and hemimetaphyseal-bone-area (HMBA) between groups with the tail bent and unbent (controls) in young and old rats at 30 and 90 days

	30 days		90 days	
	Control (n = 4)	Bent tail (n = 4)	Control (n = 4)	Bent tail (n = 4)
Young				
HEA ( $\text{mm}^2 \pm \text{SEM}$ )	0.053 $\pm$ 0.123	0.095 $\pm$ 0.123	0.007 $\pm$ 0.138	0.418 $\pm$ 0.415*
HMA ( $\text{mm}^2 \pm \text{SEM}$ )	0.098 $\pm$ 0.160	-0.138 $\pm$ 0.0055	0.278 $\pm$ 0.196	-0.265 $\pm$ 0.097*
HEBA (% $\pm$ SEM)	1.450 $\pm$ 2.560	-15.125 $\pm$ 3.726†	-1.400 $\pm$ 2.920	-18.725 $\pm$ 1.188‡
HMBA (% $\pm$ SEM)	0.625 $\pm$ 1.331	-1.875 $\pm$ 8.306	-0.275 $\pm$ 1.094	-22.35 $\pm$ 2.610‡
Old				
HEA ( $\text{mm}^2 \pm \text{SEM}$ )	0.020 $\pm$ 0.090	0.323 $\pm$ 0.144	-0.023 $\pm$ 0.274	0.580 $\pm$ 0.288
HMA ( $\text{mm}^2 \pm \text{SEM}$ )	0.010 $\pm$ 0.086	-0.140 $\pm$ 0.218	0.110 $\pm$ 0.132	-0.123 $\pm$ 0.086
HEBA (% $\pm$ SEM)	0.575 $\pm$ 4.906	-6.400 $\pm$ 3.968	-8.050 $\pm$ 6.655	-11.750 $\pm$ 4.010
HMBA (% $\pm$ SEM)	0.675 $\pm$ 3.205	4.200 $\pm$ 7.594	-4.450 $\pm$ 5.641	-5.650 $\pm$ 1.441

\*  $p < 0.05$

†  $p < 0.01$

‡  $p < 0.001$

**Table IV.** Mean ( $\pm$  SD) number of osteoclasts in the hemiepiphysis of the seventh tail vertebra of young and old rats with the tail bent and the control groups for 30 and 90 days

	HE*	30 days		90 days	
		Bent tail (n = 4)	Control (n = 4)	Bent tail (n = 4)	Control (n = 4)
Young	Distr	3.13 $\pm$ 0.48	2.88 $\pm$ 0.75	3.25 $\pm$ 1.04	2.75 $\pm$ 0.96
	Compr	3.0 $\pm$ 1.08	3.0 $\pm$ 0.58	3.13 $\pm$ 0.63	2.63 $\pm$ 1.03
Old	Distr	0	0.13 $\pm$ 0.25	0	0
	Compr	0.13 $\pm$ 0.25	0	0.13 $\pm$ 0.25	0

\* HE, hemiepiphysis; Distr, distracted or right side of controls; Compr, compressed or left side of controls

(Table IV). In old rats osteoclasts were seldom observed: the difference between young and old groups was significant ( $p < 0.001$ ).

## DISCUSSION

Quantification of the stress applied to the tail vertebrae has been attempted by changing the number of vertebrae in the loop and by measuring the forces required to close the loop.<sup>16</sup> Reliable estimates of the load applied to each vertebra are difficult because of the geometry of the system with alternating elastic (disc) and stiff (vertebral) elements. The bending force applied to the system has its major effect on the elastic segment in which the annulus fibrosus showed distraction on the convex side and infolding on the concave side. It is fundamental to the understanding of our model to establish whether the bending forces are transmitted to the vertebrae. A transverse fracture of the hypertrophic chondrocyte layer is a consistent finding in experimental physeal distraction or in mechanical overload which causes progressive tilt of the epiphysis.<sup>7,17,18</sup> This change was seen in the vertebrae of all young rats in our 14-loop model. This confirms that tensile stresses were transmitted to the vertebrae and were sufficient to produce changes in the growth plate. It seems reasonable to assume that symmetrical compressive strains are present on the concave side.

In older rats a greater force was needed to close a tail loop of 14 vertebrae (Table I), but no fracture was observed. It could be that the absence of the hypertrophic and calcified cartilage cell layers makes the resting growth plate more resistant to mechanical stresses. The growth in length of the vertebrae in the young rats during the experiment makes it even more difficult to quantify the mechanical stresses.

The statement that "compressive load strengthens the bone" is generally accepted by orthopaedic surgeons and is based on Wolff's law.<sup>1,2</sup> More recently, mathematical models have simulated bone structure and its response to variations of mechanical strains.<sup>19-21</sup> In the bent-tail model the increased trabecular density in the compressed hemiepiphysis can only be explained in terms of remodelling in the two corresponding hemivertebrae by osteoclasts and osteoblasts. Increased trabecular density can result from

reduced resorption or accelerated apposition. The number of osteoclasts did not show significant differences between corresponding hemiepiphyses in the experimental or the control groups. This implies that the response of living bone to altered compressive strains may be mediated by osteoblasts producing increased synthesis of bone matrix; this was confirmed by the increased uptake of tetracycline in the compressed epiphyses.

In another model used by Mueller<sup>22</sup> and later by Chamay and Tschantz<sup>23,24</sup> to investigate the effects of mechanical forces on bone, overload was induced in the dog ulna by resection of a segment of radial diaphysis. Both fatigue fractures and adaptive hypertrophy of bone were seen, the latter being mediated by activation of periosteal osteoblasts.

When a bone is bent there is a differential electric charge on its surfaces, and this piezoelectric effect may be the signal to activate bone cells.<sup>25,26</sup> The response of bone cells to a mechanical stimulus may be mediated by a biomechanical pathway.<sup>27</sup> A further mechanism of adaptation of bone to stress could result from haemodynamic changes induced in the bone. The close relationship between the haemodynamic flow in bones and appositional activity<sup>28,29</sup> has been shown by injection techniques in the study of fracture repair.<sup>30</sup>

The transverse fissure at the level of the hypertrophic cells layer has the same significance as a fatigue fracture of the bone, as reported by Storey and Feik.<sup>16,31</sup> Comparing young and old rats, it was evident that mechanical forces produced changes in the fast proliferating growth plate cartilage, but no effects were seen in the resting plate of old rats. The observed reduction of the hemiepiphyseal area of the compressed side is related to the mechanical effect on cartilage modelling, and the increased trabecular density to the stimulated activity of osteoblasts.

No benefits in any form have been received or will be received from a commercial party related directly or indirectly to the subject of this article.

## REFERENCES

1. Wolff J. Über die innere Architektur der Knochen und ihre Bedeutung für die Fräne von Knochenwachstum. *Virchows Arch* 1870;Bd 50.
2. Wolff J. *Das Gesetz der Transformation der Knochen*. Berlin: Verlag von August Hirschwald, 1892.
3. Frost HM. Skeletal structural adaptations to mechanical usage (SATMU): 1. Redefining Wolff's law: the bone modelling problem. *Anat Rec* 1990;226:403-13.

4. **Frost HM.** A chondral modelling theory. *Calcif Tissue Int* 1979;28: 181-200.
5. **El Haj AJ, Minter SL, Rawlinson SC, Suswillo R, Lanyon LE.** Cellular responses to mechanical loading in vitro. *J Bone Miner Res* 1990;5:923-32.
6. **Skerry TM, Bitensky L, Chayen J, Lanyon LE.** Loading-related reorientation of bone proteoglycan in vivo: strain memory in bone tissue? *J Orthop Res* 1988;6:547-51.
7. **Tschantz P, Taillard W, Ditesheim PJ.** Epiphyseal tilt produced by experimental overload. *Clin Orthop* 1977;123:271-9.
8. **Rubin CT, Lanyon LE.** Regulation of bone formation by applied dynamic loads. *J Bone Joint Surg [Am]* 1984;66-A:397-402.
9. **Rubin CT, Lanyon LE.** Regulation of bone mass by mechanical strain magnitude. *Calcif Tissue Int* 1985;37:411-7.
10. **Pollard AW, Feik SA, Storey E.** Remodelling of bone and bones: effects of translation and strain on transplants. *Br J Exp Pathol* 1984; 65:655-70.
11. **Feik SA, Storey E.** Joint changes in transplanted caudal vertebrae. *Pathology* 1982;14:139-47.
12. **Feik SA, Storey E.** Remodelling of bone and bones: growth of normal and transplanted caudal vertebrae. *J Anat* 1983;136:1-14.
13. **Hsu S-M, Raine L, Fanger H.** Use of avidin-biotin-peroxidase complex (ABC) in immunoperoxidase techniques: a comparison between ABC and unlabeled antibody (PAP) procedures. *J Histochem Cytochem* 1981;29:577-80.
14. **Brookes M.** *The blood supply of bone.* London, Butterworths, 1971: 1-338.
15. **Trias A, Fery A.** Cortical circulation of long bones. *J Bone Joint Surg [Am]* 1979;61-A:1052-9.
16. **Storey E, Feik SA.** Remodelling of bone and bones: effects of altered mechanical stress on caudal vertebrae. *J Anat* 1985;140:37-48.
17. **de Pablos J, Cañadell J.** Experimental physal distraction in immature sheep. *Clin Orthop* 1990;250:73-80.
18. **Fishbane BM, Riley LH Jr.** Continuous transphyseal traction: experimental observations. *Clin Orthop* 1978;136:120-4.
19. **Cowin SC, Firoozbakhsh K.** Bone remodelling of diaphyseal surfaces under constant load: theoretical predictions. *J Biomech* 1981;14: 471-84.
20. **Fyhrie DP, Carter DR.** A unifying principle relating stress to trabecular bone morphology. *J Orthop Res* 1986;4:304-17.
21. **Huiskes R, Weinans H, Grootenboer HJ, et al.** Adaptive bone-remodeling theory applied to prosthetic-design analysis. *J Biomech* 1987;20:1135-50.
22. **Mueller W.** Experimentelle Untersuchungen über mechanisch bedingte Umbildungsprozesse am wachsenden und fertigen Knochen und ihre Bedeutung für die Pathologie des Knochens, insbesondere die Epiphysenstörungen bei rachitisähnlichen Erkrankungen. *Bruns Beitr Klin Chir* 1922;127:251-90.
23. **Chamay A.** Mechanical and morphological aspects of experimental overload and fatigue in bone. *J Biomech* 1970;3:263-70.
24. **Chamay A, Tschantz P.** Mechanical influences in bone remodelling: experimental research on Wolff's law. *J Biomech* 1972;5:173-80.
25. **Becker RC, Basset CAL, Bachmann CH.** Bioelectrical factors controlling bone structure. In: Frost H. M. ed. *Bone. Biodynamics.* Boston: Little-Brown, 1964:209-32.
26. **Basset CAL.** Biophysical principles affecting bone structure. In: Bourne GH, ed. *The biochemistry and physiology of bone.* New York: Academic Press, 1971:1-76.
27. **Brighton CT, Fisher JR, Levine SE, et al.** The biochemical pathway mediating the proliferative response of bone cells to a mechanical stimulus. *J Bone Joint Surg [Am]* 1996;78:1337-47.
28. **Trueta J, Morgan JD.** The vascular contribution to osteogenesis. I. Studies by the injection method. *J Bone Joint Surg [Br]* 1960;42-B: 97-109.
29. **Trueta J, Little K.** The vascular contribution to osteogenesis. II. Studies with the electron microscope. *J Bone Joint Surg [Br]* 1960; 42-B:367-76.
30. **Rhineland FW.** The normal microcirculation of diaphyseal cortex and its response to fracture. *J Bone Joint Surg [Am]* 1968;50-A:784-800.
31. **Storey E, Feik SA.** Remodelling of bone and bones: effects of altered mechanical stress on anlagen. *Br J Exp Pathol* 1982;63:184-93.